Mon. Not. R. Astron. Soc. **281,** 339–347 (1996)

The rotation curve of the Galaxy obtained from planetary nebulae and AGB stars

L. H. Amaral,[1] R. Ortiz,[1,2] J. R. D. Lépine[1] and W. J. Maciel[1]

[1]*Instituto Astronômico e Geofísico da USP, Av. Miguel Stefano 4200, 04301-904 São Paulo, SP, Brazil*
[2]*Departamento de Física, UFES, Campus Universitario, 29060-900 Vitoria, ES, Brazil*

Accepted 1996 February 16. Received 1996 January 12; in original form 1995 June 13

ABSTRACT

The rotation curve of the Galaxy is obtained from a sample of planetary nebulae and asymptotic giant branch (AGB) stars. The AGB stars are OH/IR stars and carbon-rich stars with large mass-loss rates, with velocities known from radio observations and distances determined from their infrared luminosity. The rotation curve exhibits a steep decrease in the solar vicinity, and a minimum at about 8.5 kpc (adopting $R_\odot = 7.9$ kpc). We fit the rotation curve with a mass distribution model of the Galaxy, based on the model for star counts in the infrared region of Ortiz & Lépine; the main components are a spherically symmetric density distribution that represents the bulge and the halo, and two exponential disc components with scalelengths 2.6 and 4.5 kpc. A good agreement is found between the star count model and the rotation curve. A minimum is observed at 8.5 kpc; possible explanations are discussed. The surface density of the disc in the solar neighbourhood is 77 $M_\odot$ pc^{-2}, not very different from the value predicted by star counts. This result implies that there is no need for a dark matter component, at least up to a radius of about 12 kpc.

Key words: stars: AGB and post-AGB – stars: kinematics – planetary nebulae: general – Galaxy: kinematics and dynamics – Galaxy: structure.

1 INTRODUCTION

Since the pioneering work by Schmidt (1965), the galactic rotation curve has been used for studies of galactic structure. Most determinations of the rotation curve are based on observations of the gaseous components of the disc (H I, CO), and rely on the assumption that the maximum velocity observed at a given longitude corresponds to the velocity of the subcentral point (see for example, Clemens 1985 and Rohlfs & Kreitschmann 1987, hereafter RK). However, in this method, perturbations of the velocity field at the subcentral point by streaming motions may affect the 'observed' rotation curve. Another difficulty is that the method of terminal velocities can only be applied inside the solar circle. It is therefore important to obtain also the rotation curve from tracers which are spread over the galactic disc, and for which individual distances can be obtained. Ideal tracers would be young massive stars, since they present velocities close to that of the surrounding gas. Among the determinations of the rotation curve based on stellar tracers, open clusters (Hron 1986), and classical Cepheids (Pont, Mayor & Burki 1994) have been used; in these cases the observations are limited by extinction in the visible.

OH/IR stars are particularly tempting candidate tracers, since they can be recognized at large distances, based solely on radio and infrared observations. A study of the sample of OH/IR stars with near-infrared photometry by Lépine, Ortiz & Epchtein (1995, hereafter LOE) compared two methods of distance determinations for these stars, and concluded that reliable distances can be obtained. Similarly a number of carbon-rich asymptotic giant branch (AGB) stars have velocities determined from CO lines, and present strong infrared emission (Loup et al. 1993). However, the AGB stars have been proved to be inhomogeneous with respect to chemical composition, age, mass and spatial distribution; clearly, a selection must be made to investigate the rotation curve.

Since Shklovskii (1956) proposed that red giant stars are the precursors of planetary nebulae, a connection between both kinds of objects has been pursued. Peimbert (1978) proposed a classification scheme for planetary nebulae

based on the abundances of chemical elements. Maciel & Dutra (1992, hereafter MD) studied a sample containing 150 planetary nebulae classified according to Peimbert's types and concluded that they represent a sequence of decreasing mass (and increasing age) from types I (thin disc planetary nebulae) to IV (halo objects). Transition objects, between the AGB and the planetary nebula phases, are very rare (see the review by Kwok 1993), so that we are forced to conclude that the transition is extremely rapid, lasting about 10^3 yr. The kinematic properties of the objects are preserved in such a short time-scale. Ortiz & Maciel (1994, hereafter OM) classified OH/IR stars into types corresponding to those suggested for planetary nebulae by Peimbert. Like type I planetary nebulae, the corresponding OM class I OH/IR stars follow the Galactic rotation curve more closely than the remaining types, because of their relatively short main-sequence lifetime. A study of the galactic rotation curve using planetary nebulae was performed by Schneider & Terzian (1983); however, they did not take into account the inhomogeneity of their sample in terms of main-sequence mass or age.

In the present work we derive the Galactic rotation curve, using young planetary nebulae, oxygen-rich and carbon-rich AGB stars as kinematic tracers. Adopting adequate selection criteria, a relatively homogeneous sample of young objects is found; the fact that different classes of objects are used allows a more uniform distribution of the tracers on the disc, since, for instance, the carbon-rich stars present a larger surface density outside the solar circle (Guglielmo et al. 1993) while the OH/IR stars are predominant in the inner parts of the Galaxy. We fit the data with two mass-distribution models of the Galaxy which only differ in their description of the bulge. One of these models is consistent with the star distribution model of Ortiz & Lépine (1993, hereafter OL), devised to predict star counts in the infrared. The nature of a minimum in the rotation curve at about 8.5 kpc from the Galactic Centre is discussed.

2 DEFINITION OF THE SAMPLE

The sample of objects that we use to determine the rotation curve of the Galaxy contains oxygen-rich (OH/IR) AGB stars, carbon-rich AGB stars and planetary nebulae. For each class of objects we adopted one or more selection criteria, so as to include objects with massive main-sequence progenitors and with relatively good distance determinations.

A catalogue of near-infrared photometry of OH/IR stars is presented by LOE. In their work the photometry and *IRAS* data are used to derive distances, based on two different methods, one using a period–luminosity and a period–ΔV (OH peak separation) relationship, and another using the absolute L or (12-μm) magnitude as a function of the colour index $K-L$. The interstellar extinction is taken into account, by using the known distribution of interstellar gas in the galactic disc. Both methods agree fairly well, but there is an uncertainty in individual distance determinations because the sources are variable and the phase at observation time is not usually known. As discussed by LOE, the $K-L$ index is an indicator of mass for OH/IR stars; we selected only objects with $K-L>1.5$. We also removed objects with $\Delta V>35$ km s^{-1} from the sample since they are probably supergiants, which do not have the same luminosity as the stars belonging to the Mira-OH/IR sequence. The radial velocities are the average value of the two OH peaks (we discarded single peak stars); the original references for OH velocities are cited in table 1 of OM; typical errors are about 1 km s^{-1}.

The carbon-rich AGB stars were selected from the catalogues of Loup et al. (1993) and of Kastner et al. (1993); these catalogues contain radial velocities obtained from CO observations. The distances are given by Loup et al., based on a constant luminosity equal to 10^4 $L_\odot$; the same method was applied to the data of Kastner et al. Like OH/IR stars, carbon-rich stars form a sequence in infrared colour diagrams which is interpreted as a sequence of mass, and the mass-loss rate is correlated with the luminosity and with the mass of the star (see Epchtein, Le Bertre & Lépine 1990). Since the mass-loss rate is presented in the catalogue by Loup, we selected objects with mass-loss rate larger than 10^{-5} $M_\odot$ yr^{-1}; this is the mass-loss rate which roughly corresponds to the limit adopted for OH/IR stars ($K-L>1.5$), according to LOE.

The kinematics of *planetary nebulae* was analysed by MD; they found that type I and possibly IIa planetary nebulae show small deviations from the rotation curve as given by Clemens (1985). In order to include only objects which presumably have high-mass main-sequence progenitors, we included only the type I planetary nebulae from the list of MD. The distances come from the catalogue by Maciel (1984); most of them are derived from a mass–radius relationship. Individual determinations, based on other astrophysical methods, were also used, according to the reference list in the catalogue. MD point out that the distances to individual planetary nebulae are uncertain by about a factor of 2; this feeling is obtained by comparing different methods. Despite the poor knowledge of the distance, they are still valid in a statistical sense. Note that the sample of planetary nebulae is a small part of our sample. Most radial velocities of planetary nebulae given in MD are from the catalogue of Schneider et al. (1983), with typical errors of less than 10 km s^{-1}.

An additional selection criterion that was applied to all the tree samples of tracers is the exclusion of objects with distance from the Galactic plane $z>200$ pc, because they may present large deviations relative to the rotation curve. The final numbers of objects in our sample are: 33 planetary nebulae; 80 OH/IR stars; and 69 carbon stars (182 objects). The distribution of the objects on the Galactic disc is shown in Fig. 1.

3 A MODEL OF MASS DISTRIBUTION

3.1 Are the H I terminal velocities explained by rotation?

Since our sample of tracers covers a limited range of Galactic radius, we make use of the H I and CO rotation velocities derived by Clemens (1985) to complete the rotation curve in the inner parts of the Galaxy. This is necessary since it does not make sense to model only a small part of the rotation curve. We consider two alternative hypotheses to interpret these data. The first one is the classical interpretation of the H I terminal velocity as a function of longitude, as being a measure of the rotational velocity at the subcentral point.

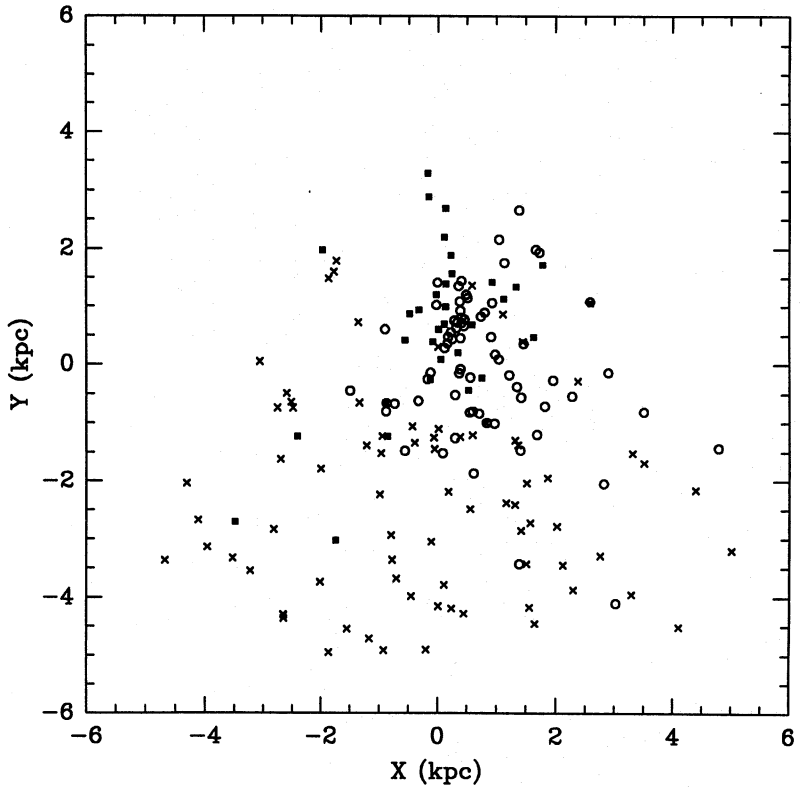

Figure 1. The distribution of objects in our sample projected on the galactic plane. The Sun is at the centre of the figure. Circles: carbon stars; crosses: OH/IR stars; squares: planetary nebulae.

This is the view adopted by Burton (1988), Clemens (1985) and Rohlfs & Kreitschmann (1987) among others. While this interpretation is generally believed to be correct for the outer parts of the Galaxy ($R > 2$ kpc), it is controversial for the inner parts. The difficulty is that the rotation curve peaks at a velocity of 250 km s^{-1} at about 300 pc, but the stellar velocity dispersion is only 120–130 km s^{-1} at the same radius. Sanders (1989) argues that the motion is predominantly circular between 200 and 1000 pc; the steep rotation gradient given by OH/IR stars (Lindqvist et al. 1989) tends to validate this view. Burton & Liszt (1993, hereafter BL) presented a radically different interpretation of the H I data, proposing that there is a global expansion of the gas in the inner 2 kpc of the Galaxy, with velocity of the order of the rotation velocity. The expansion would produce a peak at about 500 pc, if interpreted as being caused by rotation. We remark, however, that such an expansion velocity as proposed by BL is not observed in other spiral galaxies (see, e.g., the velocity fields presented by van Woerden 1978) and would be difficult to explain. Furthermore, the rotation curve of the Andromeda nebula presents a peak at about 0.5 kpc, similar to that of the Galaxy, and in that case there is no doubt that it is caused by rotation (Rubin & Kent Ford 1970).

A more realistic interpretation of the observed velocities is given by Binney et al. (1991). According to these authors, the potential is dominated by a bar, and the clouds have elongated orbits which intercept one another, giving rise to a shock. In this case the average circular velocity is lower than the observed velocity. In order to take into account this possibility, the second hypothesis that we consider is a constant mass/luminosity model like that of Kent (1992; see his fig. 3). It is likely that our first hypothesis gives an upper limit to the mass of the bulge, and our second hypothesis a lower limit. As discussed by Kent (his section 4), a maximum circular velocity of 212 km s^{-1} could be in agreement with the observed velocity dispersion. We must recognize that the mass distribution of the bulge is still uncertain. Both infrared brightness distribution and star counts in the direction of the bulge are dominated by the disc, and disc subtraction and extinction corrections are model dependent. The model of OL reproduces correctly the star counts in Baade's window but is very different from the model proposed by Kent (1992), which is based on observations of the brightness distribution. The present paper does not pretend to contribute to the debate on the nature of the rotation curve within 2 kpc of the centre, and leaves the question open, by considering two extreme cases.

3.2 The main mass components

The rotation curve gives us valuable information about the mass distribution in the Galaxy, but the nature of the main mass components must be inferred from star counts or from brightness distribution models. Visible star counts are unable to probe the inner parts of the Galaxy, owing to the heavy obscuration by interstellar dust. Detailed models are now available which reproduce simultaneously star counts in the near-infrared and the *IRAS* mid-infrared data (Wainscoat et al. 1992; OL). Since these models reproduce

correctly star counts in all directions in the Galaxy, over a large range of limiting magnitudes, we believe that they provide a better description of the Galaxy than models which aim to describe the integrated light, at only one wavelength. The same expressions used by OL to describe stellar densities are adapted here to represent the mass distribution.

The main components are as follows.

(1) A spherically symmetric component, represented by the Hernquist (1990) function

$$\rho(R)=\frac{M_b}{2\pi}\frac{a}{R}\frac{1}{(R+a)^3}, \quad (1)$$

where M_b is the total mass and a the scalelength. Both hypotheses discussed above are conveniently described by this expression, using different values of M_b and a. We remarked that the constant mass/luminosity model of Kent (1992) is well fitted by equation (1) (see Section 4.3).

(2) A stellar disc with surface mass density represented by the sum of two exponential laws

$$\sigma(R)=\sigma_1 \exp(-R/\alpha_1)+\sigma_2 \exp(-R/\alpha_2), \quad (2)$$

where α_1 and α_2 are the scalelengths of the disc components, assumed to be 2.6 and 4.5 kpc respectively, following the suggestion by OL. The use of these two exponential laws is not very different from a single exponential law with an intermediary scalelength of 3.5 kpc, as adopted for instance by Wainscoat et al. (1992). We use the infinitesimal thin-disc approximation developed by Freeman (1970) to obtain the gravitational potential.

(3) Part of the mass of the disc is in the form of gas. The gas distribution in the disc was included by fitting an expression to the gas surface density from CO and H II data (Sanders et al. 1984). The thin-disc approximation was also used in this case. We found that the observed gas density can be represented by a sum of three components:

$$\sigma(\mathrm{R})=\sigma_0 e^{-(pR)^2}+\frac{a_1R^2}{(b_1^2+R^2)^{5/2}}+\frac{a_2R^2}{(b_2^2+R^2)^{5/2}}. \quad (3)$$

The above constants are: $\sigma_0=300\ \mathrm{M_\odot\ pc^{-2}}$; $p=0.90\ \mathrm{kpc^{-1}}$; $a_1=12\,250\ \mathrm{kpc^3\ M_\odot\ p^{-2}}$; $b_1=4.20$ kpc; $a_2=-1475\ \mathrm{kpc^3\ M_\odot\ p^{-2}}$; $b_2=2.25$ kpc. It is preferable to use this expression instead of a polynomial as it tends to 0 for large values of R. The expression includes a factor of 1.4 to allow for the presence of helium. We considered the gas distribution to be known; the only parameters which were allowed to vary were M_b and a of the bulge, and σ_1 and σ_2 of the disc. The Galactic potential as a function of R is obtained from the mass distribution by using Poisson's equation, and the rotation curve is obtained by equating the centripetal force with the gravitational force.

Besides the main components already described, we tested additional components to attempt to fit the minimum in the rotation curve around 8.5 kpc, as later discussed. One alternative component is a second spherical distribution of mass, intended to reproduce the dark matter. An expression similar to equation (1) was adopted, with different values of M_b and a. Another test that we made was to introduce a spiral arm perturbation in the potential. The spiral potential shape is described by an expression similar to that proposed by Contopoulos & Grosbol (1988), modified to include a 4-arms component:

$$\phi_p(r,\theta)=AR e^{(-\beta R)}\left\{\cos\left[\frac{m\ln(R)}{\tan(i)}-m(\theta-\gamma)\right]+\alpha\cos\left[\frac{2m\ln(R)}{\tan(i)}-2m(\theta-\gamma)\right]\right\}, \quad (4)$$

where θ is the galactocentric angle, A is the amplitude of the spiral perturbation, β^{-1} the scalelength of the spiral, i is the pitch angle, $m=2$, α is the relative strength of the 2- and 4-arms components, and γ is a phase angle. The existence of a 4-spiral-arms pattern with pitch angle $i=14°$ which reproduces the observed tangential directions is discussed by OL: in a separate paper (Amaral & Lépine 1996, in preparation) the self-consistency of a superposition of 2- and 4-spiral-arm components in the potential of the Galaxy is examined. In the present work our purpose is only to show that a reasonable choice of the parameters in equation (4) is able to reproduce some of the observed features of the rotation curve, but not all of them. It should be noted in Fig. 1 that, as seen from the Galactic Centre, most data points at distances larger than $\mathrm{R_\odot}$ are situated within a small range of θ, so that we can approximate $\theta=0°$ in equation (4). The effect of the spiral velocity field near the Sun is local and must be distinguished from the true rotation curve.

4 RESULTS AND DISCUSSION

The Galactic rotation velocity of an object, $\Theta(R)$ is calculated by the expression

$$\Theta(R)=\left[\frac{V_{\mathrm{LSR}}}{\sin(l)\cos(b)}+\Theta_\odot\right]\frac{R}{\mathrm{R_\odot}}, \quad (5)$$

where V_{LSR} is its velocity with respect to the local standard of rest, l and b its galactic coordinates and $\Theta_\odot$ the galactic rotation velocity at $R=\mathrm{R_\odot}$. In this work we adopt $\mathrm{R_\odot}=7.9$ kpc and $\Theta_\odot=184\ \mathrm{km\ s^{-1}}$, following OL and Rohlfs & Kreitschmann (1987). Although the IAU recommended in 1985 the use of the values $\mathrm{R_\odot}=8.5$ kpc and $\Theta_\odot=220\ \mathrm{km\ s^{-1}}$, the preferred values of $\mathrm{R_\odot}$ have declined in the last decade, and consequently also the values of $\Theta_\odot$, since their ratio is tied to the Oort constants. The presently accepted values of $\mathrm{R_\odot}$ are 7–8 kpc, as reviewed, e.g., by Reid (1989) and by Fich & Tremaine (1991). The velocity of the LSR recommended by Kuijken & Tremaine (1994) is $180\ \mathrm{km\ s^{-1}}$, very close to our adopted value. However, we also made tests with the 1985 IAU values, as later discussed.

Note that equation (5) is only valid if the LSR rotation around the Galactic Centre is purely circular. The value of u_0, the velocity of the LSR receding from the Galactic Centre, is still a matter of debate. Blitz & Spergel (1991) argue in favour of $u_0=14\ \mathrm{km\ s^{-1}}$. Kuijken & Tremaine (1994: equation 18) concluded that u_0 is very small ($-1\pm9\ \mathrm{km\ s^{-1}}$). In any case, we also analysed the data considering $u_0=10\ \mathrm{km\ s^{-1}}$.

The sample defined in Section 2 contains 182 objects in the range $4<R<12$ kpc, for which individual determina-

tions of $\Theta(R)$ were achieved. These results were grouped into radial bins, 1 kpc wide, in which the rotation velocity is represented by the average of individual determinations of $\Theta(R)$ in that bin. Some smoothing is obtained by calculating the 1-kpc averages every 0.5 kpc.

Fig. 2 shows the rotation curve as obtained from our sample. The circles are our data for planetary nebulae, OH/IR stars, and carbon stars. The crosses are individual determinations from the sample of Clemens (1985), who used H I data for $0 < R < 2.5$ kpc, and CO data for $2.5 < R < 7.9$ kpc (corrected here for $R_\odot = 7.9$ kpc). These data are useful for fitting the mass model in the inner parts of the Galaxy, where planetary nebulae and AGB stars are absent in our sample, and for comparison in the region of overlap with our data. Fig. 3 is like Fig. 2, except that our second hypothesis is used to describe the rotation curve near the centre.

4.1 The errors

We take into account two different types of errors. One type of uncertainty is well accounted for by the standard error of the mean of the rotation velocities in each bin. Among the causes of the observed dispersion of the data is the variability of the OH/IR stars and carbon-rich AGB stars, and the random phase of the photometric measurements. The errors on distances produce errors in rotation velocities, from equation (5). Besides the random errors, we may have systematic errors if the scale of absolute magnitudes as a function of colour index adopted by LOE is incorrect. In order to illustrate the effect of systematic errors, we present in Fig. 4 three sets of data points: (1) the same data of Fig. 2, (2) a set obtained by increasing the distances of the objects in our sample by 30 per cent, and then computing their new galactocentric distances and their rotation velocities (3) a set obtained similarly with distances decreased by 30 per cent. We consider that 30 per cent is a reasonable estimation of possible systematic error on distance. The error bars that we present in Figs 2 and 3 are the quadratic sum of the standard error of the mean in each bin and of the velocity range owing to systematic errors as given in Fig. 4, for each bin. Some authors present error bars of individual objects for both axes. We think that our procedure is preferable, since the errors in each axis are not independent; the errors in the rotation velocity are mainly owing to the uncertainty in the distance. We did not include the contribution of the uncertainty in $R_\odot$.

We verified that if we add a radial velocity $u_0 = 10$ km s^{-1} to the LSR, the aspect of the rotation curve does not change appreciably, although the rotation velocities of individual stars inside a bin may present changes. This is because our

The data points at 4.5 and 5 kpc, with velocities of 170 and 180 km s^{-1}, respectively, situated well below the rotation curve of the gas may possibly be affected by larger errors than indicated, although our results seem to be confirmed by other authors, as discussed later. These points are distant (by about 3 kpc) OH/IR stars, and an error larger than 30 per cent in their distance would produce a large effect on the position relative to the subcentral point, and consequently a large error in the rotation velocity of each star.

4.2 Comparison with previous works: the minimum at 8.5 kpc

A number of interesting features can be observed in Figs 2 and 3. The rotation curve presents a broad maximum around $R = 6.0$ kpc, a sharp minimum at 8.5 kpc, and an enhancement around 10 kpc. The existence of a minimum at 8.5 kpc has been observed by other authors, but its nature has not been fully discussed. This minimum is expected from Oort's constants ($-A - B = \mathrm{d}\Theta/\mathrm{d}R = -5$ km s^{-1})

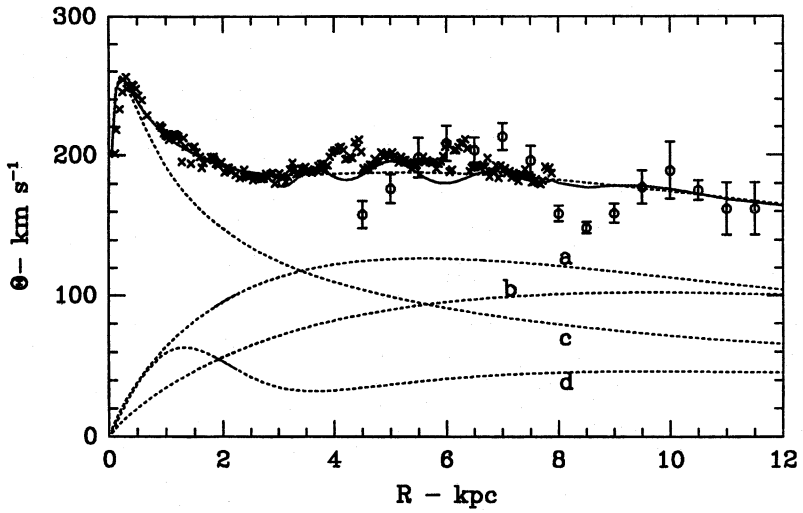

Figure 2. The rotation curve of the Galaxy. Interstellar gas data by Clemens (1985) are shown (crosses). The average data of our sample, which contains planetary nebulae, OH/IR stars and carbon stars, are represented by circles, for $R > 4$ kpc. The error bars include the standard error of the mean in each bin and an estimation of systematic errors (see text). The uppermost dotted line is the model of mass distribution of the Galaxy if the peak at about 300 pc is interpreted as being due to rotation (hypothesis 1); the components of the model are also shown: (a) thin disc with 2.6-kpc scalelength; (b) thin disc with 4.5-kpc scalelength, (c) bulge, (d) gas. The solid line represents the mass model plus a model for the spiral arm velocity field (see text).

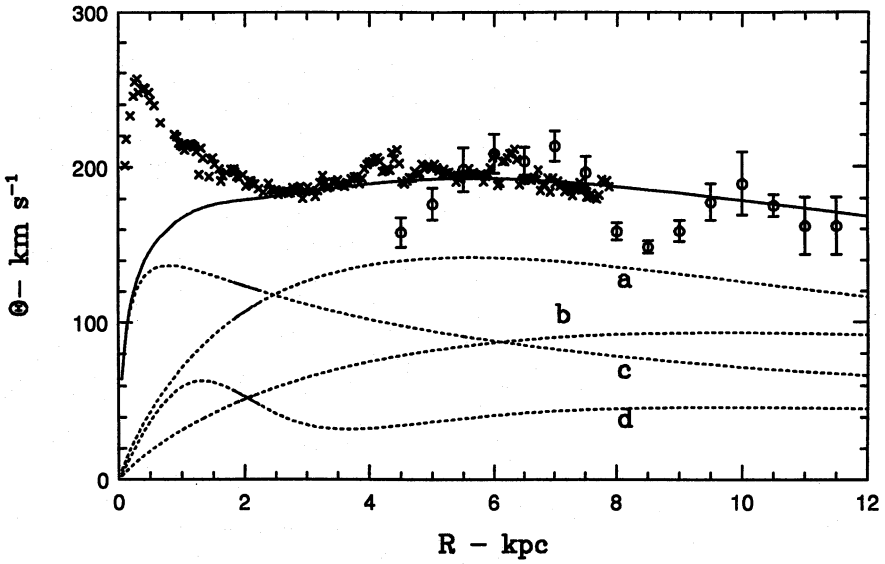

Figure 3. The rotation curve of the Galaxy, as in Fig. 2. In this figure the constant mass/luminosity model of Kent (1992) was adopted for the bulge (hypothesis 2). The solid line represents the mass model, without spiral arm perturbation.

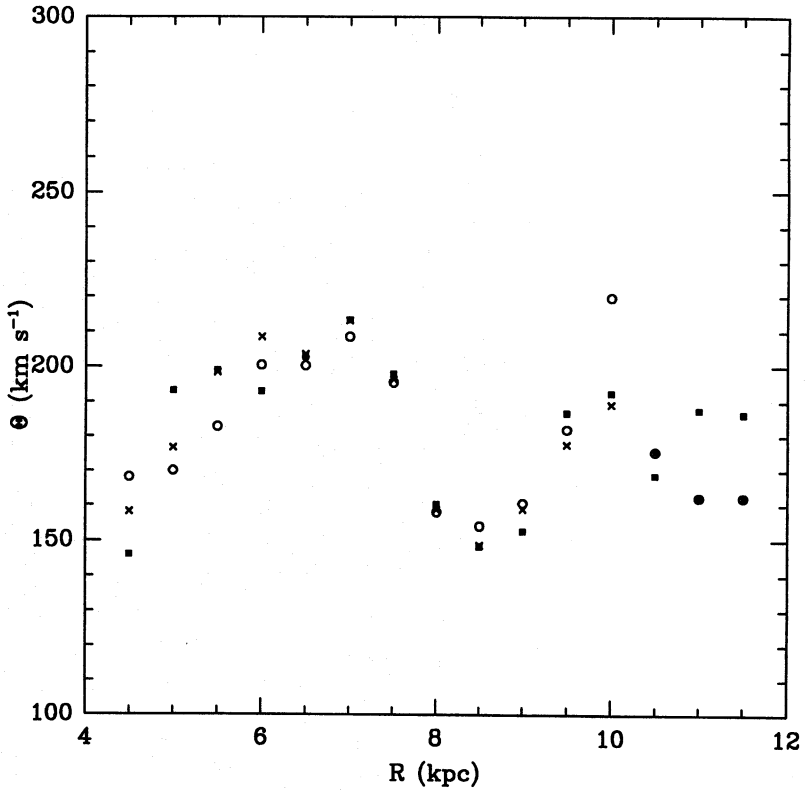

Figure 4. The effect of systematic errors in distance on the rotation curve of the Galaxy. Crosses represent the average rotation velocities in each Galactic radius bin (the same data used as shown in Fig. 2). Filled squares are the average data in each bin with the distances of all objects of the sample increased 30 per cent. Open circles denote the same for distances decreased 30 per cent.

which give a negative gradient of rotation velocity near the Sun, while at large distances the rotation curve seems to rise (e.g. Blitz 1979). The minimum can be observed in the rotation curve based on H II regions by Georgelin & Georgelin (1976), at the same radius after correction for our $R_\odot$. The 21-cm data displayed by RK shows many points below the rotation curve at 8.5 kpc, but they are ignored by the interpolating spline in their fig. 5. However, the magnitude of the gradient or the depth of the minimum that we obtain are greater than indicated by most previous works; we find a decrease in the rotation velocity of about 50 km s^{-1} between 7.0 and 8.5 kpc.

We performed a series of tests, varying $R_\odot$, u_0 and the LSR rotation velocity, to test if the 8.5-kpc minimum could be an artefact caused a particular choice of the constants involved in the model. The rotation curve obtained with the 1985 IAU values, $R_\odot = 8.5$ kpc, $\Theta_\odot = 220$ km s^{-1}, is shown in Fig. 5. It can be remarked that the discrepancy between the gas data and our data near 5 kpc becomes larger when the IAU LSR velocity is adopted. In all of these tests the minimum at 8.5 kpc remained about the same. Results similar to ours were obtained from a study of open clusters by Hron (1986); we must take into account the difference in the assumed solar rotation velocity and in $R_\odot$. Hron (his fig. 8) also finds a maximum at about $R - R_\odot = -2$ kpc, with a sharp decrease on both sides; the amplitude between the maximum and the minimum at about $R - R_\odot = 1$ kpc is also of the order of 50 km s^{-1}. However, the rotation curve fitted by Hron to his data produces a strong smoothing of these variations. The results obtained from classicial Cepheids by Pont et al. (1994) are more difficult to compare, since they do not plot the data directly; they present a smoothed curve in their fig. 6 and the residuals in fig. 10, but the residuals present important variations. The main characteristics are similar to our results, although with a smaller amplitude of variation. The results of Hron and of Pont et al., like ours, seem to indicate that the rotation velocity obtained from stars is below the gas rotation velocity given by Clemens (1985) at about $R - R_\odot = -3$ kpc.

We compare in Fig. 6 our results with those of Brand & Blitz (1994, hereafter BB). The authors use H II regions and reflection nebulae to extend the rotation curve to large galactocentric distances. In this figure, the line is the same as that shown as a dotted line in Fig. 2 and represents the model fitting of our data. It can be seen that the data of BB present a large scattering, a concentration of points below the average curve at 9 kpc, and are in rough agreement with our data. We recalculated the rotation velocities of the

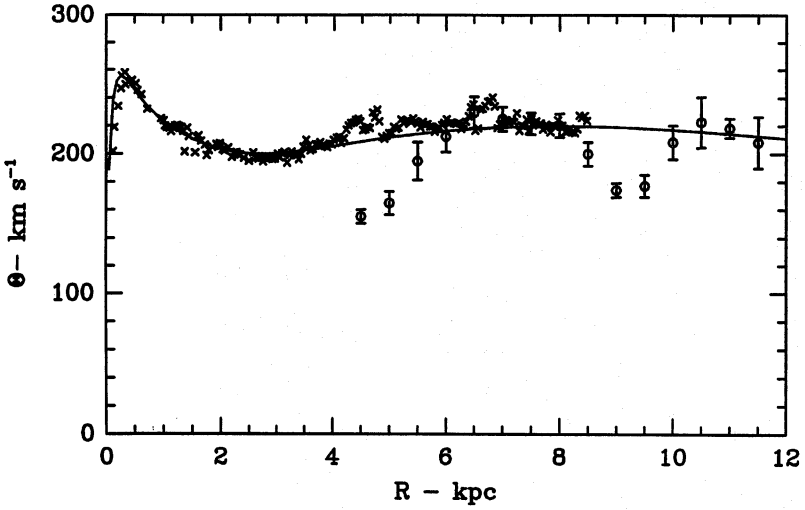

Figure 5. The rotation curve of the Galaxy, as in Fig. 2, assuming the 1985 IAU recommended values $R_\odot = 8.5$ kpc, $\Theta_\odot = 220$ km s^{-1}.

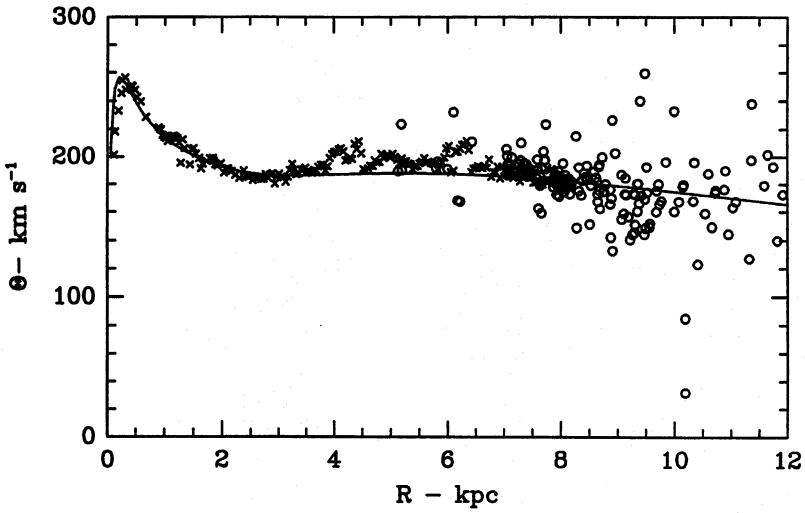

Figure 6. Comparison of our model with the data of Brandt & Blitz (1994). The line represents our model of mass distribution, similar to the dotted line in Fig. 2. Interstellar gas data by Clemens (1985) are shown (crosses). The H II regions and reflection nebulae of the sample of BB, corrected for our value of the rotation velocity of the LSR, are represented by open circles.

sample of BB, using our adopted solar rotation velocity of 184 km s^{-1}. As a result the data of BB do not present a clearly rising velocity for $R > 10$ kpc, as stated in their paper. The agreement between our sample and the sample of BB does not improve significantly for $\Theta_\odot = 184$ km s^{-1} compared with $\Theta_\odot = 220$ km s^{-1}. Our results indicates that the Galaxy possibly presents a flat rotation curve in its external part, like many other spiral galaxies; certainly an upper limit to the contribution of dark matter would be strongly affected by the parameter $\Theta_\odot$.

4.3 Model fitting

We fitted the model for the Galaxy described in Section 3 to the interstellar gas data (for $R < 5.0$ kpc), and to our data (for $R > 5.0$ kpc). First, we fitted the data by a model without spiral arms. The result of this modelling is shown in Fig. 2 (dotted line) and in Fig. 3 (solid line), for the two hypotheses considered in this paper; the contribution of each component described in Section 3 is also shown (a quadratic sum of the velocities of each component must be made to obtain the total velocity). The parameters obtained for the spherically symmetric component are $M_b = 1.24 \times 10^{10}$ $M_\odot$ and $a = 0.203$ kpc (hypothesis 1) or $M_b = 1.40 \times 10^{10}$ $M_\odot$ and $a = 0.8$ kpc (hypothesis 2); the parameters of the disc are $\sigma_1 = 591$ $M_\odot$ pc^{-2} and $\sigma_2 = 221$ $M_\odot$ pc^{-2} (hypothesis 1) or $\sigma_1 = 740$ $M_\odot$ pc^{-2} and $\sigma_2 = 185$ $M_\odot$ pc^{-2} (hypothesis 2). The corresponding values of the mass of the disc components are $M_{2.6} = 2.51 \times 10^{10}$ $M_\odot$ and $M_{4.5} = 2.82 \times 10^{10}$ $M_\odot$ (hypothesis 1) or $M_{2.6} = 3.14 \times 10^{10}$ $M_\odot$ and $M_{4.5} = 2.35 \times 10^{10}$ $M_\odot$ (hypothesis 2); the surface density of matter in the solar vicinity is 78 $M_\odot$ pc^{-2} in both cases. This last value is in good agreement with star counts, since we obtain 51 $M_\odot$ pc^{-2} from the model of OL (40 $M_\odot$ pc^{-2} for the stars and 11 $M_\odot$ pc^{-2} for the gas); the model of OL does not take into account white dwarfs which could amount to about 20 per cent of the total mass (e.g. Bahcall & Soneira 1980). The broad maximum in the curve between 3.5 and 7.5 kpc owing to the disc component with scalelength 2.6 kpc can be seen (component 'a'); a disc with larger scalelength (4.5 kpc for component 'b') produces a maximum at a much larger radius. This result confirms the importance of the 2.6-kpc disc, as revealed by star counts.

The minimum in the rotation curve at 8.5 kpc could not be reproduced by a 'dark matter' component, as described in Section 3 (not shown in Fig. 2). Any reasonable dark matter distribution would have a slowly increasing contribution, producing a flat curve, but would not fit a sharp minimum. The model of the Galaxy by Kent (1992), with the addition a dark halo, like our model, was unable to fit the minimum at about 8.5 kpc, clearly visible in his fig. 3.

When spiral arms are invoked the picture does not change much. The solid line in Fig. 2 represents the rotation curve with the spiral perturbation. The perturbation is calculated along the locus of subcentral points, for $R < R_\odot$, and along the line connecting the Galactic Centre in the Sun, for $R > R_\odot$. As already discussed, we do not expect to observe in the data the wave-like variations calculated from the model, since the objects of our sample are spread all over the galactic plane, while the model is calculated along a line. For the objects outside the solar circle, however, this is an acceptable approximation.

The parameters of the spiral component are $i = 14°$, $m = 2$, $A = 100$ km^2 s^{-2} kpc^{-1}, $\alpha = 1$, $\gamma = 0°$. The sharp discontinuities which appear at about 2.7, 6.2 and 8 kpc are resonances associated with the 2- and 4-arms components; the details of the dynamical model are discussed by AL. Our results suggest that the enhancement observed at about 10 kpc in the rotation curve could be a local perturbation associated with the Perseus spiral arm. The amplitude of the spiral potential perturbation that we present in Fig. 2 (solid line) corresponds to 7 per cent of the axisymmetric Galactic potential. If we consider that only the gas is contributing to the density contrast, this would correspond to a contrast in density of about 80 per cent for the gas. As can be seen from Fig. 2, a spiral perturbation amplitude 2 to 3 times larger would produce a better fit to the data. This would imply that not only the gas but also a fraction of the stars contribute to the density contrast. Alternatively, one should look for different kinds of velocity perturbation, instead of the usual density waves, to explain the minimum at 8.5 kpc.

The non-axisymmetric distortions of the Galactic disc near the Sun, as proposed by Blitz & Spergel (1991), do not predict a minimum in the rotation velocity near 8.5 kpc, but instead a smoothly decreasing quadrupole contribution. We remark that such distortions are not very different from what we call a 4-arm spiral perturbation, and that a simple spiral arm model, as discussed by AL, also predicts a motion of the LSR receding from the Galactic Centre, like the model of Blitz & Spergel.

5 CONCLUSION

We have investigated the rotation curve of the Galaxy using AGB stars and planetary nebulae. The characteristics of the rotation curve are found to be in agreement with the mass distribution derived from the main stellar population components which describe star counts. We suggest that the minimum observed in the curve at 8.5 kpc is not strictly a feature of the galactic potential. It could be a local effect of the spiral arm perturbation, but in this case the amplitude of the perturbation would be surprisingly large. Our results show that large-mass AGB stars and planetary nebulae follow the Galactic rotation curve relatively closely, confirming the results by MD for planetary nebulae. This also confirms that a sample of massive AGB stars can be selected by using criteria such as the $K - L$ colour index or the mass-loss rate. We expect that with the future completion of a deep whole-sky survey at 2.2 μm, the number of AGB stars with well-determined distances will increase considerably; for instance all the known OH/IR stars (about 1700) will have their near-infrared magnitudes measured. This will allow a more detailed study of the rotation curve and an investigation of the differences between the velocity of the gas and that of the stars.

ACKNOWLEDGMENTS

This work was partially supported by FAPESP under grant 91/2315-8, and by CNPq.

REFERENCES

Bahcall J. N., Soneira R. M., 1980, ApJS, 44, 73
Binney J., Gerhard O. E., Stark A. A., Bally J., Uchida K. I., 1991,

MNRAS, 252, 210
Blitz L., 1979, ApJ, 231, L115
Blitz L., Spergel D. N., 1991, ApJ, 370, 205
Brand J., Blitz L., 1994, A&A, 275, 67 (BB)
Burton W. B., 1988, in Verschuur G. L., Kellermann K. I., eds, Galactic and Extragalactic Radio Astronomy. Springer-Verlag, New York, p. 295
Burton W. B., Gordon M. A., 1978, A&A, 63, 7
Burton W. B., Liszt H. S., 1993, A&A, 274, 765 (BL)
Clemens D. P., 1985, ApJ, 295, 422
Contopoulos G., Grosbol P., 1988, A&A, 197, 83
Epchtein N., Le Bertre T., Lépine J. R. D., 1990, A&A, 227, 82
Fich M., Tremaine S., 1991, ARA&A, 29, 409
Freeman K. C., 1970, ApJ, 160, 811
Georgelin Y. M., Georgelin Y. P., 1976, A&A, 49, 57
Guglielmo F., Epchtein N., Le Bertre T., Fouqué P., Hron J., Kerschbaum F., Lépine J. R. D., 1993, A&AS, 99, 31
Hernquist L., 1990, ApJ, 356, 359
Hron J., 1986, A&A, 176, 34
Kastner J. H., Forveille T., Zuckerman B., Omont A., 1993, A&A, 275, 163
Kent S. M., 1992, ApJ, 387, 181
Kuijken K., Tremaine S., 1994, ApJ, 421, 178
Kwok S., 1993, ARA&A, 31, 63
Lépine J. R. D., Ortiz R., Epchtein N., 1995, A&A, 299, 453 (LOE)
Lindqvist M., Winnberg A., Habing H. J., Matthews H. E., Olnon F. M., 1989, in Morris M., ed., IAU Symp. No. 136, The Center of the Galaxy. Kluwer, Dordrecht, p. 503
Loup C., Forveille T., Omont A., Paul J. F., 1993, A&AS, 99, 291
Maciel W. J., 1984, A&AS, 55, 253
Maciel W. J., Dutra C. M., 1992, A&A, 262, 271 (MD)
Ortiz R., Lépine J. R. D., 1993, A&A, 279, 90 (OL)
Ortiz R., Maciel W. J., 1994, A&A, 287, 552 (OM)
Peimbert M., 1978 in Terzian Y., ed., IAU Symp. No. 76, Planetary Nebulae. Reidel, Dordrecht, p. 215
Pont F., Mayor M., Burki G., 1994, A&A, 285, 415
Reid M. J., 1989, in Morris M., ed., IAU Symp. No. 136, The Center of the Galaxy. Kluwer, Dordrecht, p. 37
Rohlfs K., Kreitschmann J., 1987, A&A, 178, 95 (RK)
Rubin V. C., Kent Ford W., Jr, 1970, ApJ, 159, 379
Sanders R. H., 1989, in Morris M., ed., IAU Symp. No. 136, The Center of the Galaxy. Kluwer, Dordrecht, p. 77
Sanders D. B., Solomon P. M., Scoville N. Z., 1984, ApJ, 276, 182
Schmit M., 1965, in Blaauw A., Schmidt M., eds, Stars and stellar systems, Galactic Structure, Vol. V. Univ. Chicago Press, Chicago, p. 513
Schneider S. E., Terzian Y., 1983, ApJ, 274, L61
Schneider S. E., Terzian Y., Purgathofer A., Perinotto M., 1983, ApJS, 52, 399
Shklovskii I. S., 1956, Astron. Zh., 33, 315
van Woerden H., 1978, in Burton W. B., ed., IAU Symposium No. 84, The Large-Scale Characteristics of the Galaxy. Reidel, Dordrecht, p. 501
Wainscoat R. J., Cohen M., Volk K., Walker H. J., Schwartz D. E., 1992, ApJS, 83, 111